LASERS

Higher-dimensional supersymmetric microlaser arrays

Xingdu Qiao[1]†, Bikashkali Midya[2,3]†, Zihe Gao[2]†, Zhifeng Zhang[1], Haoqi Zhao[1], Tianwei Wu[2], Jieun Yim[2], Ritesh Agarwal[2], Natalia M. Litchinitser[4], Liang Feng[2,1]*

The nonlinear scaling of complexity with the increased number of components in integrated photonics is a major obstacle impeding large-scale, phase-locked laser arrays. Here, we develop a higher-dimensional supersymmetry formalism for precise mode control and nonlinear power scaling. Our supersymmetric microlaser arrays feature phase-locked coherence and synchronization of all of the evanescently coupled microring lasers—collectively oscillating in the fundamental transverse supermode—which enables high-radiance, small-divergence, and single-frequency laser emission with a two-orders-of-magnitude enhancement in energy density. We also demonstrate the feasibility of structuring high-radiance vortex laser beams, which enhance the laser performance by taking full advantage of spatial degrees of freedom of light. Our approach provides a route for designing large-scale integrated photonic systems in both classical and quantum regimes.

The rapid development of integrated photonics, with continuous effort to push the limit of integration density, offers a solution to the future scaling of integrated photonic networks and devices. However, the wave nature of light gives rise to fundamentally inevitable mutual coupling between photonic elements that are closely packed in an array. Control of mutual coupling is thus the key to phase locking all of the elements and further driving them to function collectively. For example, coherence and synchronization are critical for high-radiance optical emitters and lasers, as the radiance scales with the number of elements only if they are mutually coherent (*1*, *2*). Integrated high-radiance sources including synchronized laser arrays (*1*–*9*) and photonic crystal lasers (*10*, *11*) are in high demand and are actively pursued for a wide range of applications, including optical communication, optical sensing, and light detection and ranging (LIDAR). Among various strategies developed to enforce mutual coherence between laser resonators, the evanescent wave coupling–based strategy—which leverages strong optical confinement (such as micro- and nanoscale resonators and waveguides) and operates in the deep subwavelength regime—is approaching the limit of integration density. A key drawback of evanescent wave coupling is its intrinsically associated energy splitting, which leads to complex mode competition and thus energy inefficiency and irregular, chaotic radiation. The alternative approaches, including anti-guided, diffractive, and antenna coupling (*3*–*6*), require delicately designed leakage of optical modes to communicate between elements, which ultimately limits their downsizing and dense packaging as well. Here, we demonstrate a formalism based on higher-dimensional supersymmetry (SUSY) to enforce phase locking and to enable coherent oscillation in a two-dimensional (2D) laser array of evanescently coupled microlasers, opening avenues for the realization of integrated high-radiance sources while maintaining individual controllability of each microlaser.

SUSY was first introduced in string and quantum field theory to unify all physical interactions in nature, including strong, electroweak, and gravitational coupling (*12*). Despite awaiting experimental validation in particle physics, the mathematic framework of SUSY has found its applications in many other branches of modern physics, ranging from nonrelativistic quantum mechanics and condensed-matter physics (*13*, *14*) to optics and photonics (*15*, *16*). SUSY is particularly powerful in tailoring mutual interactions in any arbitrary lattice of evanescently coupled elements, regardless of its complexity and size. With the unbroken SUSY, for example, the lattice Hamiltonian (where couplings are represented by the off-diagonal elements) can be transformed into a new superpartner Hamiltonian with a reduced matrix dimension, which shares almost the same eigenspectrum except for the disappearance of the original fundamental mode. This characteristic has enabled a series of photonic functionalities such as effective mode control, selection, and creation (*15*–*21*), which has facilitated phase-locked 1D laser arrays when strategically performed in a non-Hermitian photonic environment (*7*–*9*). Nevertheless, the factorization technique used in supersymmetric transformation applies only to the Hamiltonians of 1D systems (*13*), which limits the scalability of SUSY photonics and hinders its further promotion into higher dimensions. Here, we have overcome this limitation and demonstrate a generic approach to higher-dimensional supersymmetric microlaser arrays. The dissipative superpartners, coupled to a 2D main laser array, enforce the evanescently coupled microlasers to phase lock and coherently oscillate in the fundamental in-phase supermode, taking the full advantage of dense integration and fulfilling the demand for integrated, high-radiance optical sources with an orders-of-magnitude enhancement in energy density.

We use a homogeneously coupled 2D array of five by five (5 × 5) identical microring lasers made of InGaAsP multiple quantum wells (Fig. 1). Considering the evanescent wave coupling between only the nearest neighbors, the main microlaser array can be represented by a tight-binding Hamiltonian

$$H = -\sum_{m,n}\left(\kappa_x a^{\dagger}_{m+1,n} a_{m,n} + \kappa_y a^{\dagger}_{m,n+1} a_{m,n} + h.c.\right) \quad (1)$$

where κ_x and κ_y denote the nearest-neighbor coupling coefficient between adjacent microrings along the x and y directions, respectively; (m, n) labels the microring sites in the (x, y) plane; $a(a^{\dagger})$ is the photon annihilation (creation) operator of the resonant modes in individual microrings; and *h.c.* denotes the Hermitian conjugate, leading to 25 transverse supermodes with closely spaced eigenfrequencies (fig. S1) (*22*). Despite many transverse supermodes, our objective is to facilitate high-radiance, single-frequency lasing in 2D space with collective in-phase oscillation in only the fundamental transverse mode, while suppressing all other supermodes.

We develop a generic approach to derive the isospectral superpartners of higher-dimensional tight-binding lattices, though the SUSY-based factorization technique is one-dimensionally constrained. The orthogonality inherently associated with the tight-binding Hamiltonian in Eq. 1 allows us to separate it in the form of a Kronecker sum

$$H = H_x \oplus H_y = H_x \otimes I_y + I_x \otimes H_y$$

where $\oplus$ and $\otimes$ denote the Kronecker sum and the tensor (Kronecker) product between matrices, respectively; H_x and H_y represent 1D systems, consisting of five coupled resonators along the x and y directions, respectively, with coupling strengths κ_x and κ_y; and I_y and I_x are 5 × 5 identity matrices (*22*). Here, the 2D isospectral superpartners can be configured using the tensor product based on two superpartners of H_x and H_y. Specifically, in contrast to nonnegligible onsite

[1]Department of Electrical and Systems Engineering, University of Pennsylvania, Philadelphia, PA 19104, USA.
[2]Department of Materials Science and Engineering, University of Pennsylvania, Philadelphia, PA 19104, USA.
[3]Department of Physical Sciences, Indian Institute of Science Education and Research, Berhampur 760010, India.
[4]Department of Electrical and Computer Engineering, Duke University, Durham, NC 27708, USA.
†These authors contributed equally to this work.
*Corresponding author. Email: fenglia@seas.upenn.edu

Downloaded from http://science.sciencemag.org/ on April 24, 2021

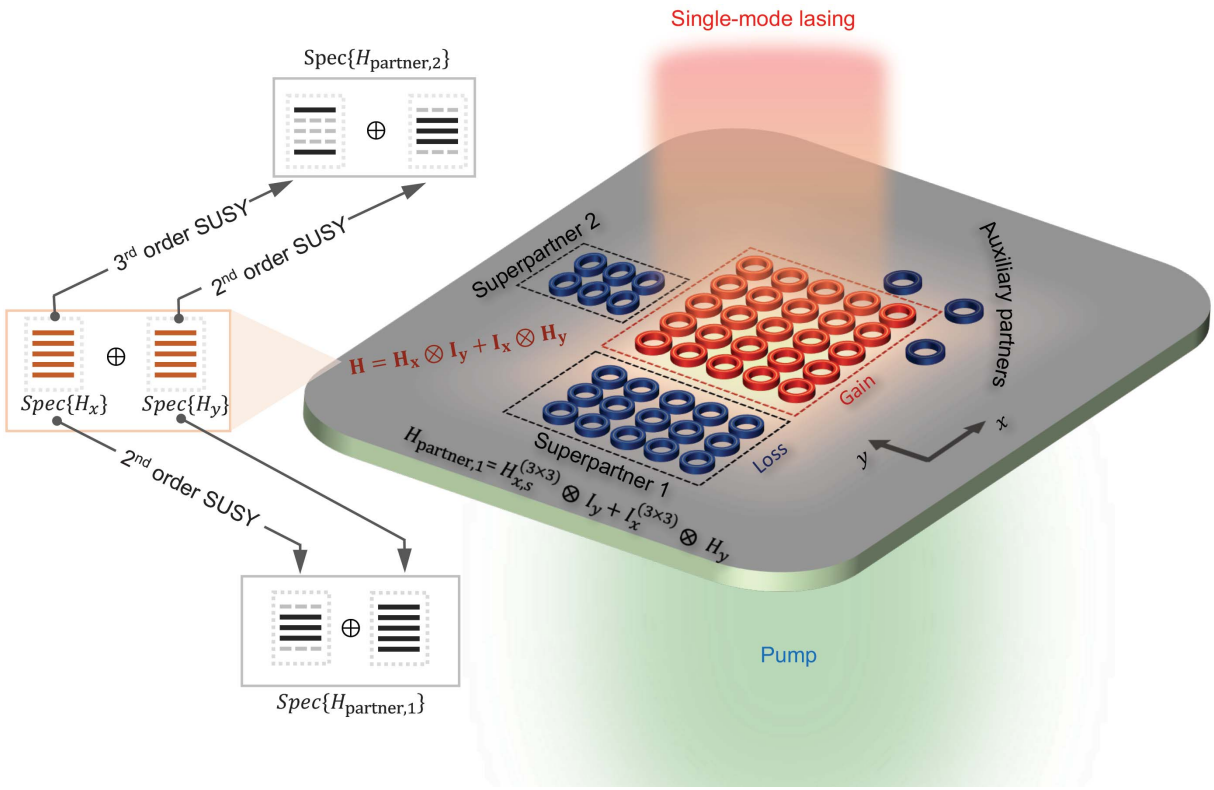

Fig. 1. A higher-dimensional supersymmetric microlaser array. The array consists of a 5 × 5 main array of evanescently coupled microring lasers (red), coupled with its two dissipative superpartner arrays and three auxiliary partner microrings (blue). The second-order SUSY transformation on H_x yields its SUSY partner $H_{x,s}^{(3\times3)}$, a 3 × 3 matrix denoting the coupling strengths in superpartner 1 in the *x* direction, which is isospectral to H_x except for the highest and lowest energy levels. A Kronecker sum between $H_{x,s}^{(3\times3)}$ and the unvaried H_y generates the Hamiltonian of superpartner 1, corresponding to an array of 3 × 5 coupled microrings. Similarly, a third-order SUSY transformation on H_x and a second-order SUSY transformation on H_y yields the Hamiltonian of superpartner 2, $H_{\text{partner},2} = H_{x,r}^{(2\times2)} \oplus H_{y,s}^{(3\times3)}$, corresponding to a 2 × 3 array. Three auxiliary partner microrings are introduced to couple to three of four remaining energy levels of *H* (*22*). Altogether, the dissipative supersymmetric and auxiliary partners are isospectral to the main array except for the lowest energy level associated with the fundamental transverse supermode, suppressing all the higher-order transverse supermodes but facilitating a high-radiance single-mode laser action operating exclusively on the fundamental in-phase supermode.

frequency detuning across the superpartner array resulting from the first-order SUSY transformation (*8*), we apply the second-order SUSY transformation that can yield a homogeneous superpartner array respecting the particle-hole symmetry and thus consisting of identical elements with the same resonant frequency compared to the main array (*9*), which is experimentally favorable, especially for a large-scale system. To create a symmetric spectrum for the superpartner, in the second-order SUSY transformation we choose to eliminate two levels with the highest and lowest frequencies in the 1D Hamiltonian (i.e., the matrix dimension of the SUSY partner of $H_{x,y}$ reduces from 5 × 5 to 3 × 3 in our case). The SUSY transformation thus leads to two superpartner arrays (*22*): a 3 × 5 array with 15 transverse modes corresponding to $H_{\text{partner},1} = H_{x,s}^{(3\times3)} \otimes I_y + I_x^{(3\times3)} \otimes H_y$, where $H_{x,s}$ is the second-order SUSY transformation of H_x, and a 2 × 3 array with six transverse modes corresponding to $H_{\text{partner},2} = H_{x,r}^{(2\times2)} \otimes I_y^{(3\times3)} + I_x^{(2\times2)} \otimes H_{y,s}^{(3\times3)}$, where $H_{y,s}$ is the second-order SUSY transformation of H_y, and $H_{x,r}$ (the residual) is an arbitrary 2 × 2 Hamiltonian that is isospectral to the energy levels originally in H_x but eliminated in achieving $H_{x,s}$. $H_{x,r}$ can also be generated by a third-order SUSY transformation of H_x by deleting three modes apart from the first and last mode (*22*). Superscripts denote the dimensions of the matrices, not to be confused with the size of the resonator array. Together with three individual auxiliary partner microrings (two of three have zero relative frequency detuning, and the frequency of the last one matches the out-of-phase supermode with the highest relative frequency among all 25 transverse modes), the spectrum of superpartners is identical to that of the main array, apart from the fundamental in-phase supermode (fig. S3) (*22*). Strategically controlled coupling of the main array with its dissipative superpartners and auxiliary partner microrings, by matching both the eigenfrequencies and mode distributions (fig. S5), therefore ensures the suppression of all but the fundamental transverse supermode, yielding efficient single-supermode lasing.

The scanning electron microscope (SEM) images of the SUSY array sample fabricated on 200-nm-thick InGaAsP multiple quantum wells (*22*) are shown in Fig. 2A. The microring resonators were patterned with an inner radius of 3 μm and a width of the waveguide of 400 nm, operating at a resonance order of N = 32 for the quasi-TE (quasi–transverse-electric) mode. To facilitate surface emission from microring lasers, an angular grating was inscribed on the inner sidewall of each microring. Emission from each scatterer in the angular grating is circularly polarized, resulting from the transverse spin in the evanescent region of the waveguide (i.e., the azimuthal and radial electric field components have a π/2 phase difference) (*23*, *24*). With the transverse spin $(|s| = 1)$, we designed the order of the angular grating as $M = N - 1 = 31$, creating phase matching for equiphase emission from all of the scatterers on a microring carrying an orbital angular momentum (OAM) of $l = 0$.

Downloaded from http://science.sciencemag.org/ on April 24, 2021

The emission spectrum of the SUSY microlaser array was characterized in addition to the emission spectra from three control experiments (Fig. 2B), all pumped optically by a nanosecond pulsed laser at the wavelength of 1064 nm (*22*). Although a single microlaser operates with the designed single-mode laser action, evanescent couplings between microlasers in a 5 × 5 array with the Hamiltonian in Eq. 1 cause energy splitting with a multimode spectrum centered at the resonance frequency of a single microlaser. In the SUSY microlaser array, selective uniform pumping of the main array with gradual intensity decay extending to its surroundings results in high-power, single-frequency lasing in the fundamental transverse supermode. In this manner, the superpartners are pumped below the lasing threshold, so they still remain dissipative, whereas the gain-loss contrast between the main array and superpartners is sufficiently low to maintain efficient couplings between them, which is equivalent to a system operating in the parity-time symmetric phase (*22*, *25*, *26*). The global mode matching with dissipative superpartners ensures the suppression of all but the fundamental supermode, which leads to high-radiance, single-frequency lasing with substantial power enhancement. The importance of the dissipative superpartners was convincingly validated by the control experiment, in which the entire SUSY microlaser array (including both the main array and the superpartners) was uniformly pumped at the same pumping intensity. Emission collected from the main array shows a multimode spectrum similar to that of the 5 × 5 array in terms of the frequencies of lasing peaks with slight power variations. In the in-phase transverse supermode, all 25 individual microlasers in the main array oscillate and contribute to power enhancement with a factor of ~25 with respect to emission from a single microlaser, as evidently shown by the light-light curves, where the slope efficiency of the SUSY microlaser array is 26.3 times as high as that of a single microlaser (Fig. 2C). Additionally, the SUSY microlaser array also exhibits a lower lasing threshold because of better optical modal overlap with the gain material.

Beyond power enhancement, the major virtue of the higher-dimensional in-phase supermode lasing is the strong 2D concentration of its emission in the far field, with ultimate energy density quadratically growing with the number of arrayed microlasers. The far-field pattern of the laser beam is a product of the far-field diffraction of the supermode and single microlaser emission (Fig. 3A). As the designed angular grating meets the condition for equiphase emission (l = 0), emissions from all scatterers in the single ring add constructively at the center of the far field as they carry the same polarization (Fig. 3B) (*22*). Specifically, the laser radiation from the 2D SUSY microlaser array exhibits a beam divergence of ~2°, compared with that of a single microlaser of ~11°. The combination of power enhancement and narrower divergence results in a two-orders-of-magnitude enhancement in energy density (Fig. 3, C and D). Each microring supports two degenerate modes (clockwise and counterclockwise circulating modes, or their hybridized interfering modes), so each transverse supermode, including the fundamental transverse supermode, carries a twofold degeneracy that contributes to laser actions (*22*). Because of the two degenerate modes being spatially offset by a phase of $\pi/2$, their associated fields are x- and y-polarized as a result from two orthogonal superpositions of the two opposite transverse spins carried by clockwise and counterclockwise modes,

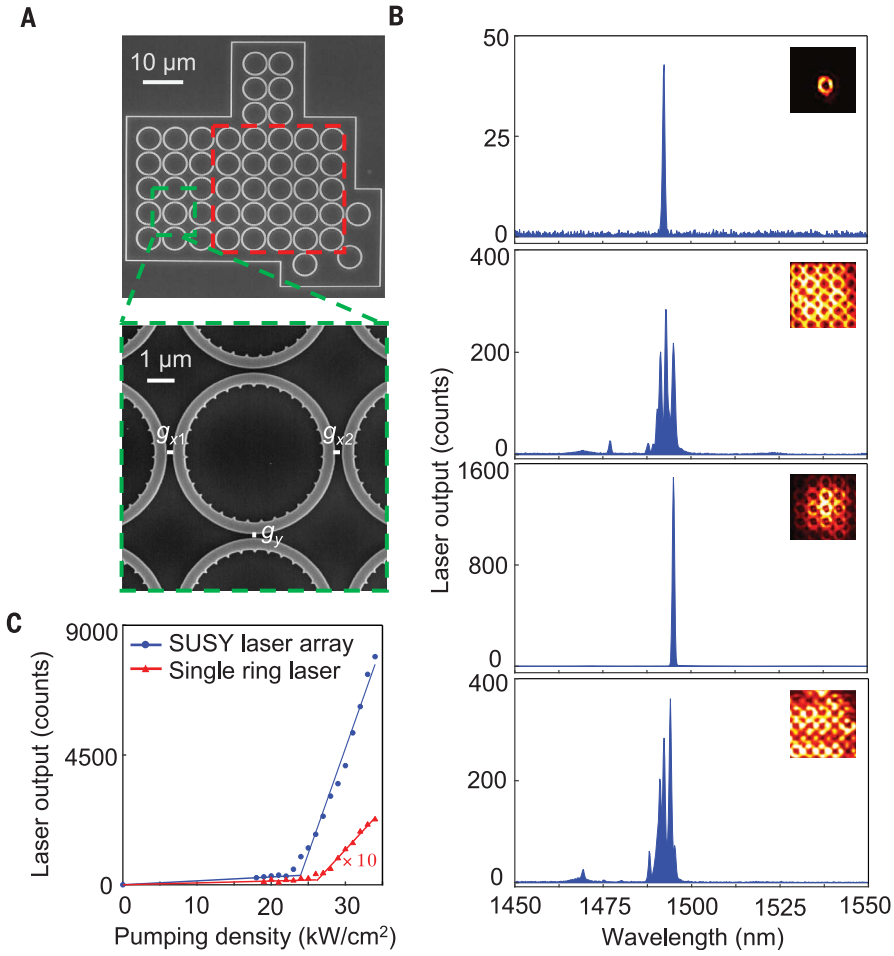

Fig. 2. Experimental characterization of the higher-dimensional supersymmetric microlaser array. (**A**) SEM images of the SUSY microlaser array. The main array is denoted by the red box, where uniform evanescent couplings are introduced with a gap of 200 nm between any pair of adjacent rings. The supersymmetric and auxiliary partners are placed in proximity to the main array, with a gap of 330 nm. The zoom-in image (bottom) shows detailed couplings in superpartner array 1: varying coupling strengths with a gap of g_{x1} = 240 nm and the other g_{x2} = 300 nm in the x direction and uniform coupling equal to that in the main array with a gap of g_y = 200 nm in the y direction. (**B**) Emission spectra, from top to bottom, of a single microring laser (single frequency lasing at 1492 nm), a 5 × 5 array of microring lasers with identical design parameters but no coupled supersymmetric and auxiliary partners, the supersymmetric microlaser array coupled with dissipative partners by selective pumping (single frequency lasing at 1495 nm), and the supersymmetric microlaser array but with uniform pumping on both the main array and partners, respectively, at the same pumping intensity of 32 kW/cm^2. The SUSY laser array lases in the longest wavelength mode among all the supermodes in the 5 × 5 array, which confirms that it is the fundamental supermode. In the two measurements for the SUSY array, only the emission from the main array is collected for a fair comparison. The insets show the corresponding emission images at the sample plane, where intensity distribution associated with the selectively pumped SUSY laser array also confirms its operation in the fundamental supermode. (**C**) Light-light curve showing the lowering of the threshold and the enhancement of lasing output (the slope efficiency) in the SUSY microlaser array compared with a single microring laser. The laser output of the single microring laser is magnified by 10× for better visualization.

Downloaded from http://science.sciencemag.org/ on April 24, 2021

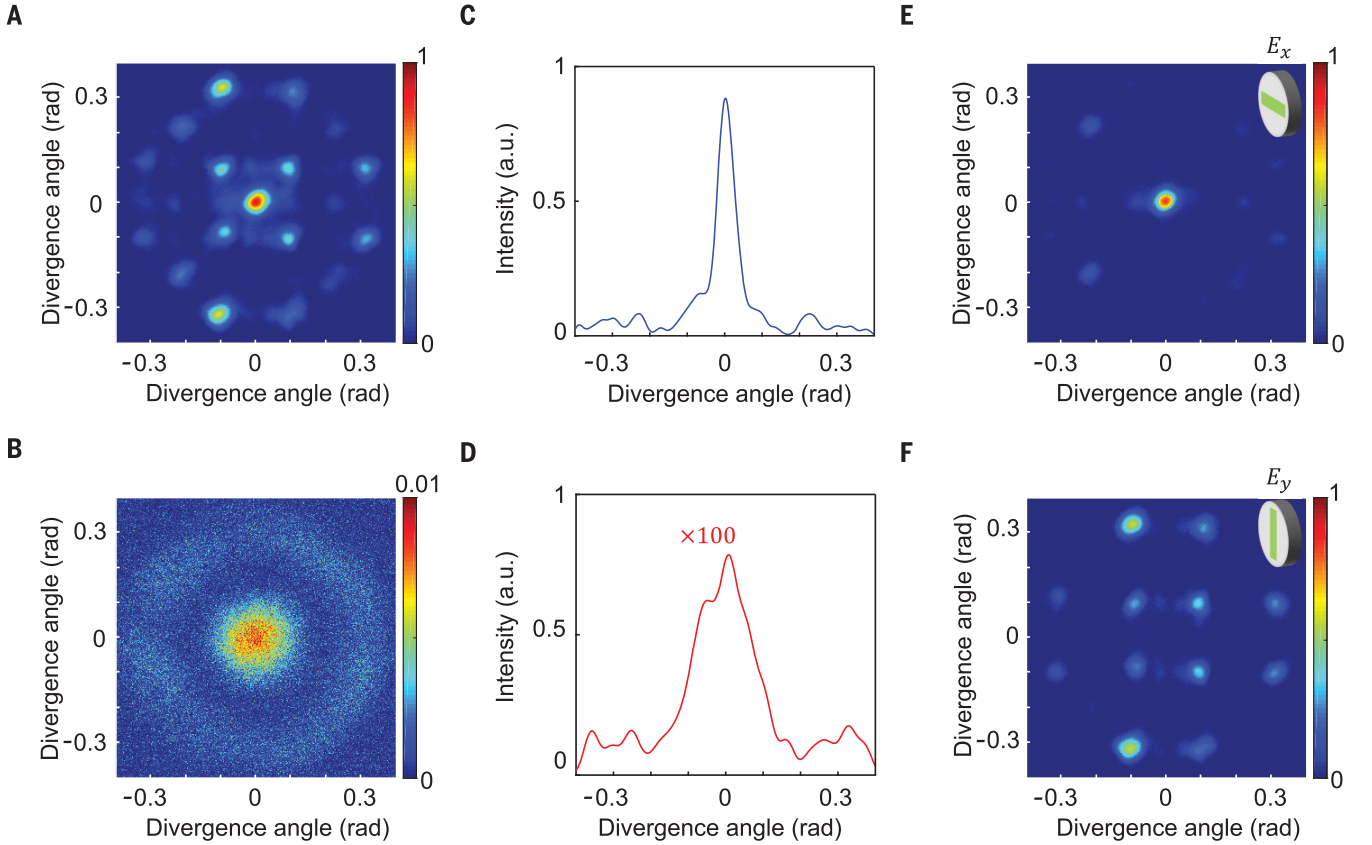

Fig. 3. Far-field characterization of laser emission from the higher-dimensional supersymmetric microlaser array. (**A** and **B**) Far-field diffraction patterns of laser emissions from the SUSY microlaser array (A) and a single microring laser (B). (**C** and **D**) The corresponding intensity distributions of laser emissions from the SUSY microlaser array (C) and single microring laser (D), both along the *x* axis, showing a small divergence of ~2° (versus divergence of ~11° for the single microlaser) and an energy concentration with a two-orders-of-magnitude enhancement in intensity associated with the laser beam from the SUSY microlaser array. Lasing intensity in (D) is magnified by 100× for better visualization. a.u., arbitrary units. (**E** and **F**) *x*- and *y*-polarized diffraction patterns of emission from the SUSY microlaser array, arising from the two degenerate modes in microrings while both oscillating in the fundamental transverse mode.

respectively. Therefore, the two degenerate modes, leading to different diffraction patterns, can be distinguished by selective measurements of the two polarization states (Fig. 3, E and F). Only the mode with the x polarization, for its in-phase characteristic, contributes to the zero-order diffraction and energy concentration at the center.

It has recently been demonstrated that single microrings offer a convenient strategy for the generation of structured light with spatially inhomogeneous phase variation and polarization distribution, such as optical vortices (*23*, *24*, *27*). Another feature of the higher-dimensional SUSY microlaser array is the ability to maintain the vectorial nature of structured light while improving the total power output. By matching the order of the angular grating with the order of the resonant mode (i.e., $M = N = 32$), the total angular momentum associated with emission becomes zero, which leads to the nonzero OAM of $l = \pm 1$ spin-orbit–locked with transverse spins of $s = \mp 1$ associated with the counterclockwise and clockwise modes in every microring, respectively (Fig. 4A). The desired phase variation and polarization distribution are collectively transferred to the laser beam emitted from the SUSY microlaser array, thereby facilitating single-frequency, high-radiance vortex lasing with a factor of 20.2 in power enhancement (Fig. 4B). Because of the phase singularity at the center of the vortex beams, energy is mainly redistributed to the first and second diffraction orders of the in-phase supermode in the far field (Fig. 4C). The phase fronts of the two vortex beams wind in opposite azimuthal directions, which creates the superposition of left- and right-handed circularly polarized fields with a continuously varying phase delay between them, leading to a vector beam with radial polarizations (*22*); along the horizontal axis, the phase delay is 0, resulting in the x-polarized field, whereas the phase delay becomes $\pm\pi$ in the vertical axis, corresponding to the y-polarized field (Fig. 4, D and E). The two vortex beams with opposite spin-orbit relations can be effectively separated using appropriate combinations of a quarter wave plate and a linear polarizer. Their associated topological charges corresponding to the OAM were characterized by performing 1D Fourier transform of the two vortex beams using a cylindrical lens (Fig. 4, G and F) (*28*). Such astigmatic transformation yields strongly deformed vortices at the focal spot with destructive interference across the 1D diffraction pattern (*22*). Only one dark fringe is clearly observed in the center area, which confirms the topological charge of OAM light of $l = \pm 1$. The orientations of the fringe with respect to the horizontal axis are correlated with the signs of the topological charges.

Our supersymmetric microlaser arrays efficiently produce high-radiance, small-divergence laser beams with an orders-of-magnitude enhancement in energy density. Developing SUSY principles into higher dimensions constitutes a powerful toolbox for effectively tailoring evanescent wave couplings in a large-scale photonic array to synchronize densely packed array elements and prescribe the desired oscillating supermode. Such strategy is generic and applicable to various platforms—for example, coupled vertical-cavity surface-emitting lasers (*2*) or coupled nanolasers (*29*, *30*). Additionally, both

Downloaded from http://science.sciencemag.org/ on April 24, 2021

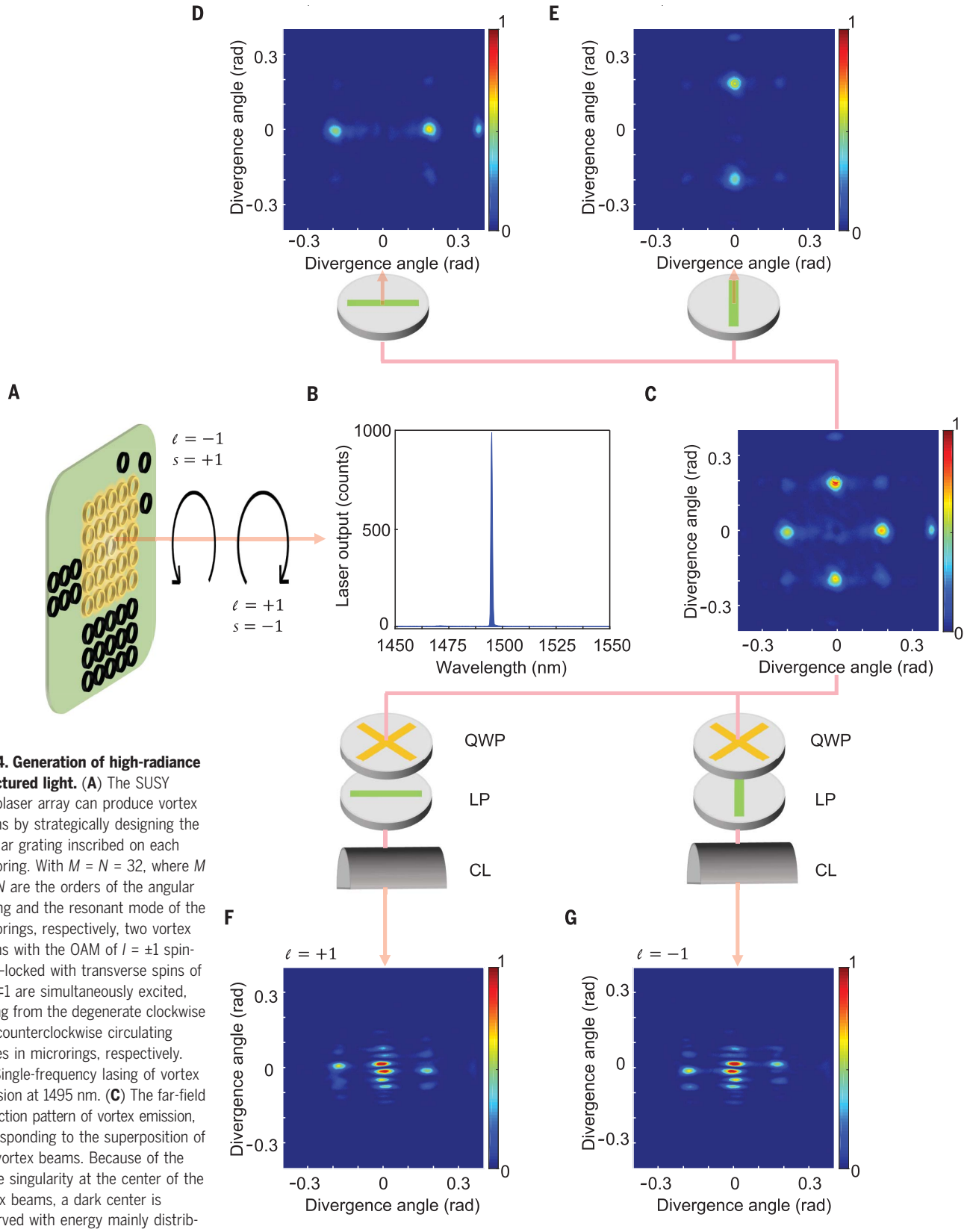

Fig. 4. Generation of high-radiance structured light. (**A**) The SUSY microlaser array can produce vortex beams by strategically designing the angular grating inscribed on each microring. With $M = N = 32$, where M and N are the orders of the angular grating and the resonant mode of the microrings, respectively, two vortex beams with the OAM of $l = \pm 1$ spin-orbit–locked with transverse spins of $s = \mp 1$ are simultaneously excited, arising from the degenerate clockwise and counterclockwise circulating modes in microrings, respectively. (**B**) Single-frequency lasing of vortex emission at 1495 nm. (**C**) The far-field diffraction pattern of vortex emission, corresponding to the superposition of two vortex beams. Because of the phase singularity at the center of the vortex beams, a dark center is observed with energy mainly distributed in the first and second diffraction orders. (**D** and **E**) *x*- and *y*-polarized diffraction patterns of superimposed vortex emissions, showing radially polarized vortex beams. (**F** and **G**) 1D diffraction patterns of the two distinct vortex beams of $l = \pm 1$, filtered by the combined quarter wave plate (QWP) and linear polarizer (LP). The 1D diffraction pattern, equivalent to the 1D Fourier transform of the far-field pattern in (C) along the *y* direction, is captured at the focal plane of a cylindrical lens (CL).

Downloaded from http://science.sciencemag.org/ on April 24, 2021

phase front and polarization of laser radiation can be spatially structured, taking full advantage of spatial degrees of freedom for deployment in the next generation classical and quantum integrated photonic systems.

REFERENCES AND NOTES

1. D. Botez, D. R. Scifres, *Diode Laser Arrays* (Cambridge Univ. Press, 2005).
2. D. F. Siriani, K. D. Choquette, in *Semiconductors and Semimetals*, vol. 86 of *Advances in Semiconductor Lasers*, J. J. Coleman, A. C. Bryce, C. Jagadish, Eds. (Elsevier, 2012), chap. 6.
3. J. R. Leger, M. L. Scott, W. B. Veldkamp, *Appl. Phys. Lett.* **52**, 1771–1773 (1988).
4. D. Botez, L. Mawst, P. Hayashida, G. Peterson, T. J. Roth, *Appl. Phys. Lett.* **53**, 464–466 (1988).
5. D. F. Siriani, K. D. Choquette, *IEEE J. Quantum Electron.* **47**, 160–164 (2011).
6. T.-Y. Kao, J. L. Reno, Q. Hu, *Nat. Photonics* **10**, 541–546 (2016).
7. R. El-Ganainy, L. Ge, M. Khajavikhan, D. N. Christodoulides, *Phys. Rev. A* **92**, 033818 (2015).
8. M. P. Hokmabadi, N. S. Nye, R. El-Ganainy, D. N. Christodoulides, M. Khajavikhan, *Science* **363**, 623–626 (2019).
9. B. Midya *et al*., *Photon. Res.* **7**, 363–367 (2019).
10. M. Yoshida *et al*., *Nat. Mater.* **18**, 121–128 (2019).
11. A. Kodigala *et al*., *Nature* **541**, 196–199 (2017).
12. M. Dine, *Supersymmetry and String Theory: Beyond the Standard Model* (Cambridge Univ. Press, 2007).
13. F. Cooper, A. Khare, U. Sukhatme, *Phys. Rep.* **251**, 267–385 (1995).
14. N. Sourlas, *Physica D* **15**, 115–122 (1985).
15. M.-A. Miri, M. Heinrich, R. El-Ganainy, D. N. Christodoulides, *Phys. Rev. Lett.* **110**, 233902 (2013).
16. M. Heinrich *et al*., *Nat. Commun.* **5**, 3698 (2014).
17. S. Longhi, *Phys. Rev. A* **82**, 032111 (2010).
18. M. Heinrich *et al*., *Opt. Lett.* **39**, 6130–6133 (2014).
19. S. Yu, X. Piao, J. Hong, N. Park, *Nat. Commun.* **6**, 8269 (2015).
20. W. Walasik, B. Midya, L. Feng, N. M. Litchinitser, *Opt. Lett.* **43**, 3758–3761 (2018).
21. S. Barkhofen, L. Lorz, T. Nitsche, C. Silberhorn, H. Schomerus, *Phys. Rev. Lett.* **121**, 260501 (2018).
22. Materials, methods, and additional information are available as supplementary materials.
23. Z. Shao, J. Zhu, Y. Chen, Y. Zhang, S. Yu, *Nat. Commun.* **9**, 926 (2018).
24. Z. Zhang *et al*., *Science* **368**, 760–763 (2020).
25. L. Feng, R. El-Ganainy, L. Ge, *Nat. Photonics* **11**, 752–762 (2017).
26. B. Peng *et al*., *Nat. Phys.* **10**, 394–398 (2014).
27. B. Bahari *et al*., *Nat. Phys.* 10.1038/s41567-021-01165-8 (2021).
28. S. N. Alperin, R. D. Niederriter, J. T. Gopinath, M. E. Siemens, *Opt. Lett.* **41**, 5019–5022 (2016).
29. K. Takeda *et al*., *Nat. Photonics* **7**, 569–575 (2013).
30. S. S. Deka, S. H. Pan, Q. Gu, Y. Fainman, A. El Amili, *Opt. Lett.* **42**, 4760–4763 (2017).

ACKNOWLEDGMENTS

Funding: We acknowledge support from the US Army Research Office (ARO) (W911NF-19-1-0249 and W911NF-18-1-0348), the National Science Foundation (NSF) (ECCS-1932803, ECCS-1842612, and OMA-1936276), and a Sloan Research Fellowship. This work was partially supported by the NSF through the University of Pennsylvania Materials Research Science and Engineering Center (MRSEC) (DMR-1720530) and was carried out in part at the Singh Center for Nanotechnology, which is supported by the NSF National Nanotechnology Coordinated Infrastructure Program under grant NNCI-1542153. **Author contributions:** B.M., L.F., and N.M.L. conceived the project. B.M. constructed the theoretical model. B.M., X.Q., Z.G., T.W., and L.F. conducted the design and performed numerical simulations. X.Q. fabricated samples. X.Q., Z.G., Z.Z., H.Z., and J.Y. performed measurements. L.F. supervised the study. All authors contributed to data analyses and manuscript preparation. **Competing interests:** The authors declare no competing interests. **Data and materials availability:** All data are available in the manuscript or the supplementary materials.

SUPPLEMENTARY MATERIALS

science.sciencemag.org/content/372/6540/403/suppl/DC1
Supplementary Text
Figs. S1 to S20

2 January 2021; accepted 24 March 2021
10.1126/science.abg3904

Downloaded from http://science.sciencemag.org/ on April 24, 2021

Science

Higher-dimensional supersymmetric microlaser arrays

Xingdu Qiao, Bikashkali Midya, Zihe Gao, Zhifeng Zhang, Haoqi Zhao, Tianwei Wu, Jieun Yim, Ritesh Agarwal, Natalia M. Litchinitser and Liang Feng

Science **372** (6540), 403-408.
DOI: 10.1126/science.abg3904

Supersymmetric switch-on

A common route to enhancing the output light from a laser system is to couple multiple lasers to form an array. However, crosstalk and interference between different modes of the individual lasers are generally detrimental to performance, leading to instabilities, and could ultimately be damaging to the laser cavities. Qiao *et al.* worked with the mathematical framework of supersymmetry, a theory developed in high-energy physics to attempt to describe the makeup and properties of particles, to design a stable two-dimensional laser array. Based on symmetry arguments, the method is scalable and could prove to be a practical platform with which to design and develop complex photonic systems.

Science, this issue p. 403

ARTICLE TOOLS http://science.sciencemag.org/content/372/6540/403

SUPPLEMENTARY MATERIALS http://science.sciencemag.org/content/suppl/2021/04/21/372.6540.403.DC1

REFERENCES This article cites 27 articles, 2 of which you can access for free
http://science.sciencemag.org/content/372/6540/403#BIBL

PERMISSIONS http://www.sciencemag.org/help/reprints-and-permissions

Use of this article is subject to the Terms of Service

Science (print ISSN 0036-8075; online ISSN 1095-9203) is published by the American Association for the Advancement of Science, 1200 New York Avenue NW, Washington, DC 20005. The title *Science* is a registered trademark of AAAS.

Copyright © 2021 The Authors, some rights reserved; exclusive licensee American Association for the Advancement of Science. No claim to original U.S. Government Works

Downloaded from http://science.sciencemag.org/ on April 24, 2021